HHS Public Access

Author manuscript

Curr Probl Diagn Radiol. Author manuscript; available in PMC 2015 November 04.

Published in final edited form as:

Curr Probl Diagn Radiol. 2008 ; 37(2): 49–56. doi:10.1067/j.cpradiol.2007.11.003.

Cardiac MR at High Field: Promises and Problems

Ahmed M Gharib[1], **Abdalla Elagha**[1], and **Roderic I Pettigrew**[2]

[1]Diagnostic Radiology Department and NHLBI, NIH, Bethesda, MD, United States

[2]NIBIB, NIH, Bethesda, MD, United States

Introduction

With the increasing availability of commercial 3 Tesla (3T) MR systems, cardiac magnetic resonance imaging (CMRI) applications at high field strength are becoming more important and rapidly evolving. The promise of increased signal-to-noise ratio (SNR) resulting from increased polarization of spins at high static magnetic field strength (B0) (1-3) opens many possibilities of improved image quality. This potential enhancement of image quality may be directly appreciated as more clear delineation of anatomic detail, or exploited to further improve spatial and/or temporal resolution (4). With increase availability of SNR at high B0 field strengths, the single loss resulting from smaller voxel size (improving spatial resolution) or using higher parallel imaging factors (5, 6) (improving temporal resolution) are more tolerable. Additionally, prolonged myocardial T1 values at higher field strengths prevents the premature fading of saturation bands (7) commonly used for tagged images employed for myocardial wall motion assessment. This prolonged T1 phenomena makes spin labeling techniques an attractive alternative for coronary (8) and possible myocardial perfusion imaging since there is less decay of the labeled spins in addition to the inherent higher SNR.

However, cardiac imaging at higher filed strength comes with many challenges. In addition to the B0 field inhomogeneity associated with high magnetic field, radiofrequency (B1) inhomogeneity (1, 3, 8-11) contributes to the degradation of image quality. The enhanced magneto-hydrodynamic effect at high field (12) may prevent reliable R wave triggering which is essential for ECG gated imaging. Further more, at high field strength, the specific absorption rate (SAR) limitations pose an additional constraint that bound the use of pulse sequences commonly applied in cardiac imaging such as steady state free precision (SSFP) sequences and prevent flexibility of pulse sequence design.

This review will focus on the current and potential future application of high magnetic field MRI for commonly used cardiac imaging applications.

Corresponding author: Ahmed Gharib, MD, National Institutes of Health, Clinical Research Center, Bldg.10, Rm.3-5340, MSC 1263, 10 Center Drive, Bethesda, MD 20892, Tel:(301) 451-8982, Fax: (301) 480-3166.

Cardiac Function and Morphology

Cardiac wall motion and ventricular function are commonly assessed using SSFP sequences at 1.5T. This technique provides an optimal contrast-to-noise ratio (CNR) between the myocardium and blood pool at a high SNR and is obtained in a relatively short breath hold allowing its practical application in the clinical setting (13, 14). Heart- lung interface induced B0 inhomogeneity (15) result in black band artifacts at high field. Such artifacts may be reduced by improving B0 homogeneity with localized linear or second-order shimming techniques and optimization of resonance frequency (16) in additionally to minimizing the repetition time (TR) (7, 17).

Michaely et. al. (18) demonstrated the feasibility of using both SSFP and segmented spoiled gradient echo (SGE) techniques at 3T for cardiac function analysis with similar accuracy compared to 1.5T. In their study 85.7% of all SSFP images at 3T demonstrated off-resonance susceptibility artifacts at the heart-lung interface, all of which were eliminated on the repeat exams after utilizing frequency scouts to determine the optimal frequency offset. They also concluded that SGE sequences benefited more from the higher magnetic field as a result of 16% increase in CNR compared to 1.5T while with SSFP imaging potential benefits were reduced by the artifacts. Tyler et. al. (19) on the other hand recommended the use of SSFP sequences because of the higher gain of SNR and CNR than SGE sequences at 3T and therefore still yield higher quality images. Undoubtedly, with the wider implementation of better shimming techniques (16) the disadvantages of using SSFP at 3T will be overcome and will become the more commonly used cine technique at 3T. The benefits of parallel imaging (acceleration factor of 2) at high field were demonstrated by Gutberlet et. al. (7) whereby there was improvement in data acquisition efficiency yielding a scan time of 8 heart beats compared to 16 heart beats without acceleration. Despite this faster acquisition, the SNR at 3T was superior to techniques used at 1.5T with and without the use of parallel imaging. The use of parallel imaging resulted in only 26% loss of SNR and 28% CNR at 3T compared to 37% and 38% at 1.5T respectively. The benefits of combining parallel imaging with high field additionally helps to counterbalance the drawbacks associated with increased RF power deposition. The shortening of scan time with less detrimental effect on image quality during cine breath hold acquisitions promotes more reliable imaging due to better patient compliance. Additionally, more cardiac phases may be acquired during a single breath hold allowing for added accurate delineation of wall motion during the entire cardiac cycle. The improved SNR may also be used to acquire higher resolution images that would potentially better depict small rapidly moving structures such as valve leaflets.

Myocardial tagging clearly benefits from higher field strength (10). The prolonged T1 time of the myocardium preserves the tags into end diastole resulting in a significant increase of CNR (187%) and SNR (87%) in this phase of the cardiac cycle where tags are usually least apparent at 1.5T (7). These results were closely matched in a more recent study (10) (figure 1). The prolonged visualization of myocardial saturation bands through out the cardiac cycle could be an valuable tool in the assessment of diastolic dysfunction which is an important distinction in the diagnosis of heart failure (20).

The use of T1 or T2 weighted techniques with inversion recovery (IR) preparation are widely used for morphological assessment of the heart. Although the sequences show improvement in SNR and CNR when applied at high field (10) the detrimental effect of B1 and B0 inhomogeneity affect uniformity of the IR preparation and reduce image quality (10). This may be overcome by using adiabatic pulses which are less sensitive to such filed inhomogeneities (21, 22). In addition to the potential spatial and temporal resolution benefits previously described, IR prepared fast spin echo (FSE) techniques may also benefit from the synergy of parallel imaging at high field by reduce the number of phase encoding steps and thereby power deposition (10). Another technique used to overcome the SAR limitations is to employ variable flip angles and hyperechoes (23). Reducing the echo train length may also allow more tolerable scan times compensated by parallel imaging and inherent signal reserve at high field without resorting to longer echo train lengths that result in increased image blurring.

Infarction and Ischemia imaging

One of the important uses of CMRI at 1.5T is in the detection of myocardial infarction utilizing delayed enhancement IR prepared techniques. It is able to differentiate infracted from hibernating myocardium with spatial resolution high enough to detect nontransmural infarcts (24-26). This image quality is further improved at high (3T) magnetic field as a result of increased SNR and CNR compared to 1.5T (10, 27). The advantage of increased CNR is the result of prolonged longitudinal relaxation of unenhanced tissues with increased field strength which leads to a higher sensitivity to injected gadolinium agents (27, 28). This may also allow for reduction of the injected dose of the gadolinium agent. The prolonged T1 time necessitates the use of longer inversion time (TI) for the IR preparation of about 330ms at 3T compared to 260ms for 1.5T (27) for optimal myocardial suppression. Additionally, the lower T1 relaxation slope at 3T compared to 1.5T allows for a more exact determination of the inversion time (27) further improving the chances of optimal CNR and thereby image quality.

The most commonly used sequence for myocardial viability imaging is an IR prepared spoiled gradient echo (IR-SGE) technique (29). The use of high field scanners improves the CNR and SNR of this sequence (10) which may be exploited to shorten scan time by complimentary use of parallel imaging (10). However, this T1 weighted sequence requires individual predetermination of TI for adequate myocardial nulling in order to achieve the desired CNR effect after contrast administration. In order to avoid these pre-scans for accurate null time determination (TI-scouts) and to achieve a consistent contrast Kellman et. al. (30) used a phase-sensitive reconstruction at 1.5T. Huber et. al. (31) showed that such technique can be implemented at 3T and accurately depict myocardial infarcts. Furthermore, they used a single-shot read out which allows for covering the entire left ventricle (9 slices) in a single breath hold as apposed to a single slice per breath hold for the more commonly used IR-SGE technique. The implementation of single-shot read out results in a 22% CNR loss at 1.5T. However, this read out technique at 3T provided a significantly higher CNR compared to similar technique and even the more conventional IR-SGE at 1.5T. Therefore, despite shortening the scan time by using a single-shot read out and avoiding the required TI-scouts there was a significant gain in CNR at 3T. This advantage should be particularly

useful for patients who cannot hold their breath well enough and patients with cardiac arrhythmias. This single-shot read out method can be applied successfully at 3T using both SGE (figure 2) (32) and SSFP (31) sequences with significant gain of CNR compared to similar techniques at 1.5T.

Myocardial perfusion MR imaging during the administration of a contrast bolus is commonly utilized for assessment of myocardial ischemia (33, 34). Due to the acquisition speed required to capture the first-pass myocardial perfusion, a saturation recovery (SR) preparation is applied to either SSFP or SGE type sequences. This provides the CNR desired for the detection of myocardial perfusion differences between images obtain during rest and stress, which in turn delineates the site of myocardial ischemia. However, in the attempt to obtain the best temporal resolution needed to better capture contrast bolus timing, the utilization of such SR prepared sequences provide poor spatial resolution. Image quality is also compromised by the use of parallel imaging due to the decreased SNR at 1.5T. Therefore, it is not surprising that perfusion imaging is significantly improved at higher magnetic field (10, 35, 36). As in viability imaging this improvement is the result of both the increased SNR and prolonged T1 time of the myocardium.

Coronary imaging

Coronary imaging by MR is one of the more challenging due to the small size of these vessels and significant motion associated with breathing and myocardial contraction. Despite these challenges coronary MRA at 1.5T has been shown to be a valuable tool for the assessment of coronary atherosclerotic disease (CAD) (37-39). Early studies demonstrated the feasibility of coronary MR angiography (CMRA) at 3T (3, 40). Compared to 1.5T the use of 3T did not show significant improvement in sensitivity or specificity for the detection of CAD, although there was an increase in SNR (40). However, the authors (40) did not exploit the full potential of higher magnetic field by pushing the limits of spatial and/or temporal resolution. With the advent of coronary CT angiography (CTA) which provides high quality images none invasively, the limits of high field coronary MRI imaging need to be further investigated in order to offer a competitive alternative without the use of radiation or nephrotoxic contrast agents.

Coronary MR imaging at 1.5T usually utilize an SSFP type sequence to obtain the highest SNR possible. Without the use of intravascular contrast agents the desired CNR between oxygenated blood and the myocardium is achieved by using T2 preparatory (T2 Prep) pulses. These techniques are implemented for both the whole-heart and targeted volume approaches. Due to B0 and B1 inhomogeneities at higher magnetic field the use both SSFP and T2 Prep pose challenges. To address such challenges an adiabatic T2 Prep (21) and SGE (3) techniques need to be used at higher magnetic fields to achieve the best image quality.

The use parallel imaging at 3T improves temporal resolution which allows for CMRA imaging using short acquisition windows. Despite the use of SGE sequences (as apposed to higher SNR allowed by SSFP used at 1.5T) the SNR is sufficient to support imaging in the systolic quiescent period (41). This may provide an opportunity for CMRA imaging in patients with tachycardia who have contraindications to the use of beta blockers necessary

for coronary CTA. Furthermore, high resolution imaging of up to 350 μm^2 is possible at 3T (figure 3) (42) which is similar to CTA resolution and unachievable at 1.5T.

While the above mentioned advances were achieved using the targeted approach, a whole-heart technique similar to CTA is probably more desirable. This whole-heart approach is feasible at 3T as it is at 1.5T using either breath holding (43, 44) or free breathing navigator gated techniques (45). Although, the whole-heart technique at 3T has been shown to be useful for the assessment of coronary artery anomalies (45), its utilization for CAD evaluation has not yet been proven to be possible as it is shown at 1.5T (38, 39). None the less, higher spatial and temporal resolution imaging using whole-heart techniques need to be explored. Similarly, black blood vessel wall imaging is feasible at 3T and is improved by using adiabatic IR preparatory pulse (22), however, the resolution limits and its application in CAD patients has not been exploited to date. The advantage of prolonged T1 time has also proven to beneficial for contrast enhanced CMRA at high magnetic field (43, 44). Further exploitation of this prolonged T1 time can potentially be used for spin labeled CMRA (8).

Flow Assessment

Phase contrast MR imaging at 1.5T is an accurate method of quantifying blood flow velocity (46, 47). Due to spatial and temporal resolution limitations its implementation has been predominantly limited to large structures such as the ventricles, valves or great vessels (48-50). Similar accuracy and precision of blood velocity measurement is achievable at high (3T) magnetic field (10, 51, 52). As a result of the increased SNR a significantly higher velocity to noise ratio is possible at 3T (10, 51, 52). This reduction of noise allows velocity measurements at 3T to tolerate a larger deviation from the preset velocity encoding especially for slow flow. Additionally, the increased SNR at high field opens the opportunity for 3-dimensional velocity maps (53-55) with three directional velocity encoding. This more comprehensive assessment of blood flow hemodynamics attainable at high field may allow for a better and more personalized understanding of congenital (figure 4) and/or acquired vascular and cardiac pathology. Furthermore, the exploitation of the higher SNR allows for the assessment of coronary blood flow using phase contrast technique (figure 5) utilizing higher spatial and temporal resolution unattainable at 1.5T (56). With coronary flow velocity measurement now possible, a true assessment of coronary flow reserve may be feasible in patients with coronary atherosclerosis without the use of contrast agents.

It is clear that cardiac MRI benefits form high magnetic field. However, several potential possibilities need to be further defined and investigated especially in patient populations. Many of the challenges of imaging at high magnetic field have been partially addressed. Further advances in sequence and coil designs are expected and will allow for continued improvement in cardiac imaging.

References

1. Singerman RW, Denison TJ, Wen H, Balaban RS. Simulation of B1 field distribution and intrinsic signal-to-noise in cardiac MRI as a function of static magnetic field. J Magn Reson. 1997; 125:72–83. [PubMed: 9245362]

2. Noeske R, Seifert F, Rhein KH, Rinneberg H. Human cardiac imaging at 3 T using phased array coils. Magn Reson Med. 2000; 44:978–982. [PubMed: 11108638]
3. Stuber M, Botnar RM, Fischer SE, et al. Preliminary report on in vivo coronary MRA at 3 Tesla in humans. Magn Reson Med. 2002; 48:425–429. [PubMed: 12210906]
4. Dougherty L, Connick TJ, Mizsei G. Cardiac imaging at 4 Tesla. Magn Reson Med. 2001; 45:176–178. [PubMed: 11146502]
5. Pruessmann KP, Weiger M, Scheidegger MB, Boesiger P. SENSE: sensitivity encoding for fast MRI. Magn Reson Med. 1999; 42:952–962. [PubMed: 10542355]
6. Sodickson DK, Manning WJ. Simultaneous acquisition of spatial harmonics (SMASH): fast imaging with radiofrequency coil arrays. Magn Reson Med. 1997; 38:591–603. [PubMed: 9324327]
7. Gutberlet M, Schwinge K, Freyhardt P, et al. Influence of high magnetic field strengths and parallel acquisition strategies on image quality in cardiac 2D CINE magnetic resonance imaging: comparison of 1.5 T vs. 3.0 T. Eur Radiol. 2005; 15:1586–1597. [PubMed: 15875193]
8. Stuber M, Weiss RG. Coronary magnetic resonance angiography. J Magn Reson Imaging. 2007; 26:219–234. [PubMed: 17610288]
9. Bottomley PA, Andrew ER. RF magnetic field penetration, phase shift and power dissipation in biological tissue: implications for NMR imaging. Phys Med Biol. 1978; 23:630–643. [PubMed: 704667]
10. Gutberlet M, Noeske R, Schwinge K, Freyhardt P, Felix R, Niendorf T. Comprehensive cardiac magnetic resonance imaging at 3.0 Tesla: feasibility and implications for clinical applications. Invest Radiol. 2006; 41:154–167. [PubMed: 16428987]
11. Nayak KS, Cunningham CH, Santos JM, Pauly JM. Real-time cardiac MRI at 3 tesla. Magn Reson Med. 2004; 51:655–660. [PubMed: 15065236]
12. Fischer SE, Wickline SA, Lorenz CH. Novel real-time R-wave detection algorithm based on the vectorcardiogram for accurate gated magnetic resonance acquisitions. Magn Reson Med. 1999; 42:361–370. [PubMed: 10440961]
13. Plein S, Bloomer TN, Ridgway JP, Jones TR, Bainbridge GJ, Sivananthan MU. Steady-state free precession magnetic resonance imaging of the heart: comparison with segmented k-space gradient-echo imaging. J Magn Reson Imaging. 2001; 14:230–236. [PubMed: 11536399]
14. Thiele H, Nagel E, Paetsch I, et al. Functional cardiac MR imaging with steady-state free precession (SSFP) significantly improves endocardial border delineation without contrast agents. J Magn Reson Imaging. 2001; 14:362–367. [PubMed: 11599059]
15. Atalay MK, Poncelet BP, Kantor HL, Brady TJ, Weisskoff RM. Cardiac susceptibility artifacts arising from the heart-lung interface. Magn Reson Med. 2001; 45:341–345. [PubMed: 11180442]
16. Schar M, Kozerke S, Fischer SE, Boesiger P. Cardiac SSFP imaging at 3 Tesla. Magn Reson Med. 2004; 51:799–806. [PubMed: 15065254]
17. Duerk JL, Lewin JS, Wendt M, Petersilge C. Remember true FISP? A high SNR, near 1-second imaging method for T2-like contrast in interventional MRI at .2 T. J Magn Reson Imaging. 1998; 8:203–208. [PubMed: 9500281]
18. Michaely HJ, Nael K, Schoenberg SO, et al. Analysis of cardiac function--comparison between 1.5 Tesla and 3.0 Tesla cardiac cine magnetic resonance imaging: preliminary experience. Invest Radiol. 2006; 41:133–140. [PubMed: 16428984]
19. Tyler DJ, Hudsmith LE, Petersen SE, et al. Cardiac cine MR-imaging at 3T: FLASH vs SSFP. J Cardiovasc Magn Reson. 2006; 8:709–715. [PubMed: 16891230]
20. Chinnaiyan KM, Alexander D, Maddens M, McCullough PA. Curriculum in cardiology: integrated diagnosis and management of diastolic heart failure. Am Heart J. 2007; 153:189–200. [PubMed: 17239676]
21. Nezafat R, Stuber M, Ouwerkerk R, Gharib AM, Desai MY, Pettigrew RI. B1-insensitive T2 preparation for improved coronary magnetic resonance angiography at 3 T. Magn Reson Med. 2006; 55:858–864. [PubMed: 16538606]
22. Priest AN, Bansmann PM, Kaul MG, Stork A, Adam G. Magnetic resonance imaging of the coronary vessel wall at 3 T using an obliquely oriented reinversion slab with adiabatic pulses. Magn Reson Med. 2005; 54:1115–1122. [PubMed: 16206145]

23. Busse RF. Reduced RF power without blurring: correcting for modulation of refocusing flip angle in FSE sequences. Magn Reson Med. 2004; 51:1031–1037. [PubMed: 15122687]
24. Ansari M, Araoz PA, Gerard SK, et al. Comparison of late enhancement cardiovascular magnetic resonance and thallium SPECT in patients with coronary disease and left ventricular dysfunction. J Cardiovasc Magn Reson. 2004; 6:549–556. [PubMed: 15137339]
25. Hunold P, Brandt-Mainz K, Freudenberg L, et al. Evaluation of myocardial viability with contrast-enhanced magnetic resonance imaging--comparison of the late enhancement technique with positronemission tomography. Rofo. 2002; 174:867–873. [PubMed: 12101477]
26. Kim RJ, Fieno DS, Parrish TB, et al. Relationship of MRI delayed contrast enhancement to irreversible injury, infarct age, and contractile function. Circulation. 1999; 100:1992–2002. [PubMed: 10556226]
27. Klumpp B, Fenchel M, Hoevelborn T, et al. Assessment of myocardial viability using delayed enhancement magnetic resonance imaging at 3.0 Tesla. Invest Radiol. 2006; 41:661–667. [PubMed: 16896300]
28. Rinck PA, Muller RN. Field strength and dose dependence of contrast enhancement by gadolinium-based MR contrast agents. Eur Radiol. 1999; 9:998–1004. [PubMed: 10370005]
29. Kim RJ, Wu E, Rafael A, et al. The use of contrast-enhanced magnetic resonance imaging to identify reversible myocardial dysfunction. N Engl J Med. 2000; 343:1445–1453. [PubMed: 11078769]
30. Kellman P, Arai AE, McVeigh ER, Aletras AH. Phase-sensitive inversion recovery for detecting myocardial infarction using gadolinium-delayed hyperenhancement. Magn Reson Med. 2002; 47:372–383. [PubMed: 11810682]
31. Huber A, Bauner K, Wintersperger BJ, et al. Phase-sensitive inversion recovery (PSIR) single-shot TrueFISP for assessment of myocardial infarction at 3 tesla. Invest Radiol. 2006; 41:148–153. [PubMed: 16428986]
32. Bauner KU, Muehling O, Wintersperger BJ, Winnik E, Reiser MF, Huber A. Inversion recovery single-shot TurboFLASH for assessment of myocardial infarction at 3 Tesla. Invest Radiol. 2007; 42:361–371. [PubMed: 17507806]
33. Al-Saadi N, Nagel E, Gross M, et al. Noninvasive detection of myocardial ischemia from perfusion reserve based on cardiovascular magnetic resonance. Circulation. 2000; 101:1379–1383. [PubMed: 10736280]
34. Nagel E, Klein C, Paetsch I, et al. Magnetic resonance perfusion measurements for the noninvasive detection of coronary artery disease. Circulation. 2003; 108:432–437. [PubMed: 12860910]
35. Ruan C, Yang SH, Cusi K, Gao F, Clarke GD. Contrast-enhanced first-pass myocardial perfusion magnetic resonance imaging with parallel acquisition at 3.0 Tesla. Invest Radiol. 2007; 42:352–360. [PubMed: 17507805]
36. Theisen D, Wintersperger BJ, Huber A, Dietrich O, Reiser MF, Schonberg SO. Myocardial perfusion imaging with Gadobutrol: a comparison between 3 and 1.5 Tesla with an identical sequence design. Invest Radiol. 2007; 42:499–506. [PubMed: 17568272]
37. Kim WY, Danias PG, Stuber M, et al. Coronary magnetic resonance angiography for the detection of coronary stenoses. N Engl J Med. 2001; 345:1863–1869. [PubMed: 11756576]
38. Sakuma H, Ichikawa Y, Chino S, Hirano T, Makino K, Takeda K. Detection of coronary artery stenosis with whole-heart coronary magnetic resonance angiography. J Am Coll Cardiol. 2006; 48:1946–1950. [PubMed: 17112982]
39. Sakuma H, Ichikawa Y, Suzawa N, et al. Assessment of coronary arteries with total study time of less than 30 minutes by using whole-heart coronary MR angiography. Radiology. 2005; 237:316–321. [PubMed: 16126921]
40. Sommer T, Hackenbroch M, Hofer U, et al. Coronary MR angiography at 3.0 T versus that at 1.5 T: initial results in patients suspected of having coronary artery disease. Radiology. 2005; 234:718–725. [PubMed: 15665221]
41. Gharib AM, Herzka DA, Ustun AO, et al. Coronary MR angiography at 3T during diastole and systole. J Magn Reson Imaging. 2007; 26:921–926. [PubMed: 17896391]

42. Ustun A, Desai M, Abd-Elmoniem KZ, Schar M, Stuber M. Automated identification of minimal myocardial motion for improved image quality on MR angiography at 3 T. AJR Am J Roentgenol. 2007; 188:W283–290. [PubMed: 17312038]
43. Bi X, Li D. Coronary arteries at 3.0 T: Contrast-enhanced magnetization-prepared three-dimensional breathhold MR angiography. J Magn Reson Imaging. 2005; 21:133–139. [PubMed: 15666400]
44. Bi X, Park J, Larson AC, Zhang Q, Simonetti O, Li D. Contrast-enhanced 4D radial coronary artery imaging at 3.0 T within a single breath-hold. Magn Reson Med. 2005; 54:470–475. [PubMed: 16032681]
45. Gharib AM, Ho VB, Rosing DR, et al. Free-breathing 3D whole-heart coronary MR angiography at 3T of coronary artery anomalies and variants: a technical feasibility study. Radiology. in press.
46. Moran PR, Moran RA, Karstaedt N. Verification and evaluation of internal flow and motion. True magnetic resonance imaging by the phase gradient modulation method. Radiology. 1985; 154:433–441. [PubMed: 3966130]
47. Zananiri FV, Jackson PC, Goddard PR, Davies ER, Wells PN. An evaluation of the accuracy of flow measurements using magnetic resonance imaging (MRI). J Med Eng Technol. 1991; 15:170–176. [PubMed: 1800748]
48. Globits S, Higgins CB. Assessment of valvular heart disease by magnetic resonance imaging. Am Heart J. 1995; 129:369–381. [PubMed: 7832111]
49. Globits S, Pacher R, Frank H, et al. Comparative assessment of right ventricular volumes and ejection fraction by thermodilution and magnetic resonance imaging in dilated cardiomyopathy. Cardiology. 1995; 86:67–72. [PubMed: 7728791]
50. Maier SE, Meier D, Boesiger P, Moser UT, Vieli A. Human abdominal aorta: comparative measurements of blood flow with MR imaging and multigated Doppler US. Radiology. 1989; 171:487–492. [PubMed: 2649924]
51. Lotz J, Doker R, Noeske R, et al. In vitro validation of phase-contrast flow measurements at 3 T in comparison to 1.5 T: precision, accuracy, and signal-to-noise ratios. J Magn Reson Imaging. 2005; 21:604–610. [PubMed: 15834905]
52. Pai VM. Phase contrast using multiecho steady-state free precession. Magn Reson Med. 2007; 58:419–424. [PubMed: 17654571]
53. Frydrychowicz A, Bley TA, Dittrich S, Hennig J, Langer M, Markl M. Visualization of vascular hemodynamics in a case of a large patent ductus arteriosus using flow sensitive 3D CMR at 3T. J Cardiovasc Magn Reson. 2007; 9:585–587. [PubMed: 17365238]
54. Frydrychowicz A, Harloff A, Jung B, et al. Time-resolved, 3-dimensional magnetic resonance flow analysis at 3 T: visualization of normal and pathological aortic vascular hemodynamics. J Comput Assist Tomogr. 2007; 31:9–15. [PubMed: 17259827]
55. Markl M, Harloff A, Bley TA, et al. Time-resolved 3D MR velocity mapping at 3T: improved navigator-gated assessment of vascular anatomy and blood flow. J Magn Reson Imaging. 2007; 25:824–831. [PubMed: 17345635]
56. Nezafat R, Stehning C, Gharib AM, et al. Improved spatial-temporal resolution MR coronary blood flow imaging at 3T. J Cardiovasc Magn Reson. 2005; 7:199–200.

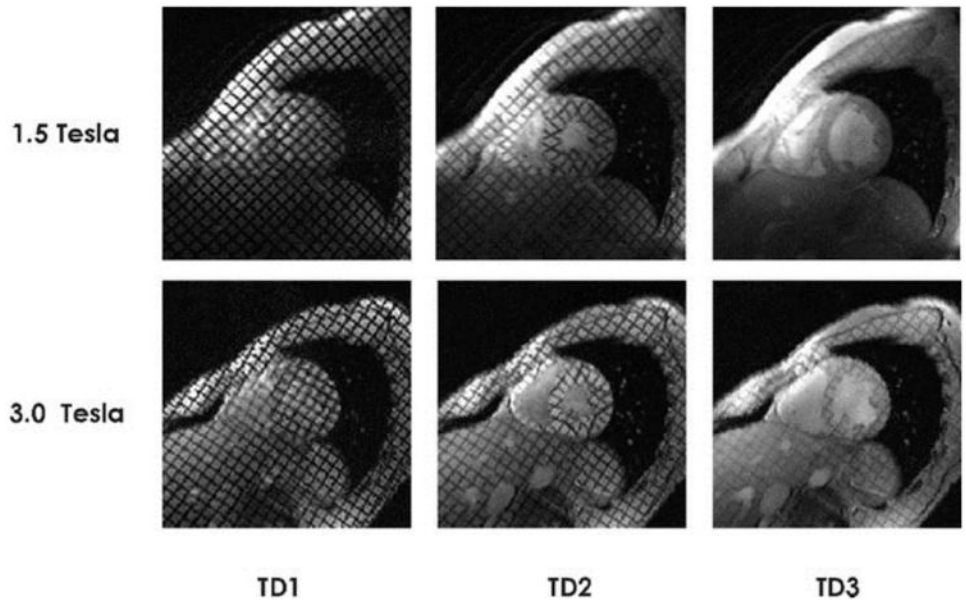

Figure 1.

Interindividual comparison of midventricular short-axis views obtained with gradient echo-based 2-D CINE tagging techniques for a healthy volunteer at 1.5 T (top) and 3.0 T (bottom) at the beginning of the cardiac cycle (trigger delay 1 = TD1), end-systole (TD2), and end-diastole (TD3). At 1.5 T, the saturation bands expired before the end of the cardiac cycle (TD3) and hence the tagging grids disappeared at approximately 75% of the RR interval. At 3.0 T, the tags were present throughout the entire heart cycle (TD1–TD3).

From: reference (10)

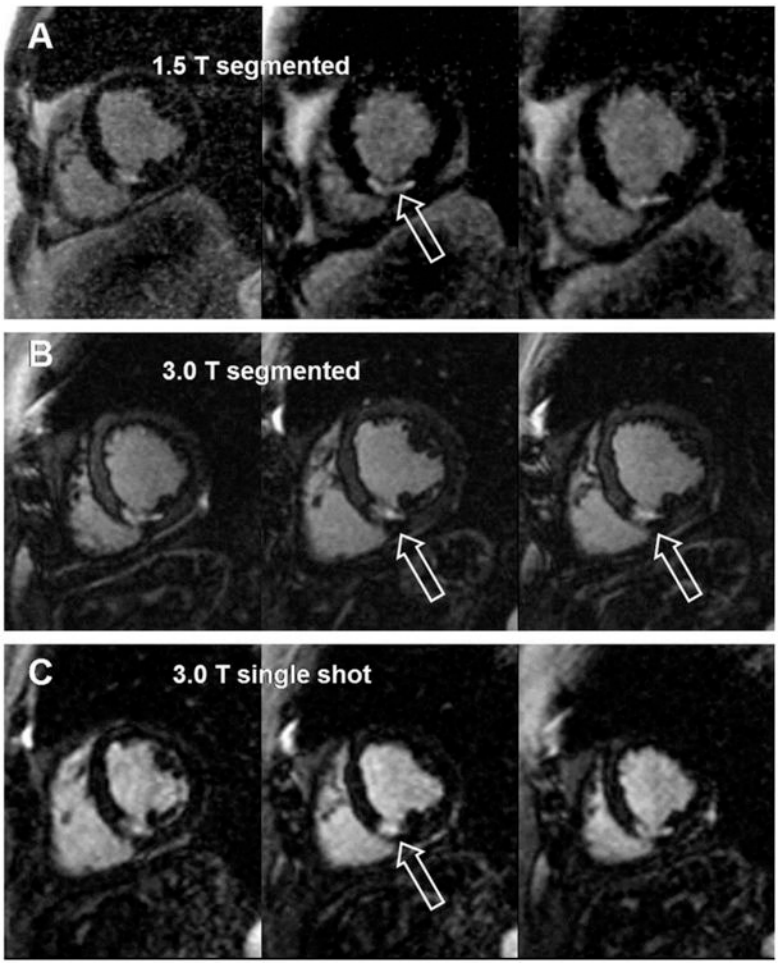

Figure 2.

Sixty-seven-year-old male patient with a subendocardial infarction in the perfusion territory of the right coronary artery and the circumflex artery. The upper 3 images were acquired with a segmented IR turboFLASH at 1.5 Tesla (A), the middle images (B) were acquired with a segmented IR turboFLASH sequence at 3.0 Tesla, and the lower 3 images (C) were acquired with a single-shot IR turboFLASH sequence at 3.0 Tesla. All images reveal hyperenhanced myocardium in the lateral, inferolateral, inferior and inferoseptal segments corresponding to myocardial infarctions.

From: reference (32)

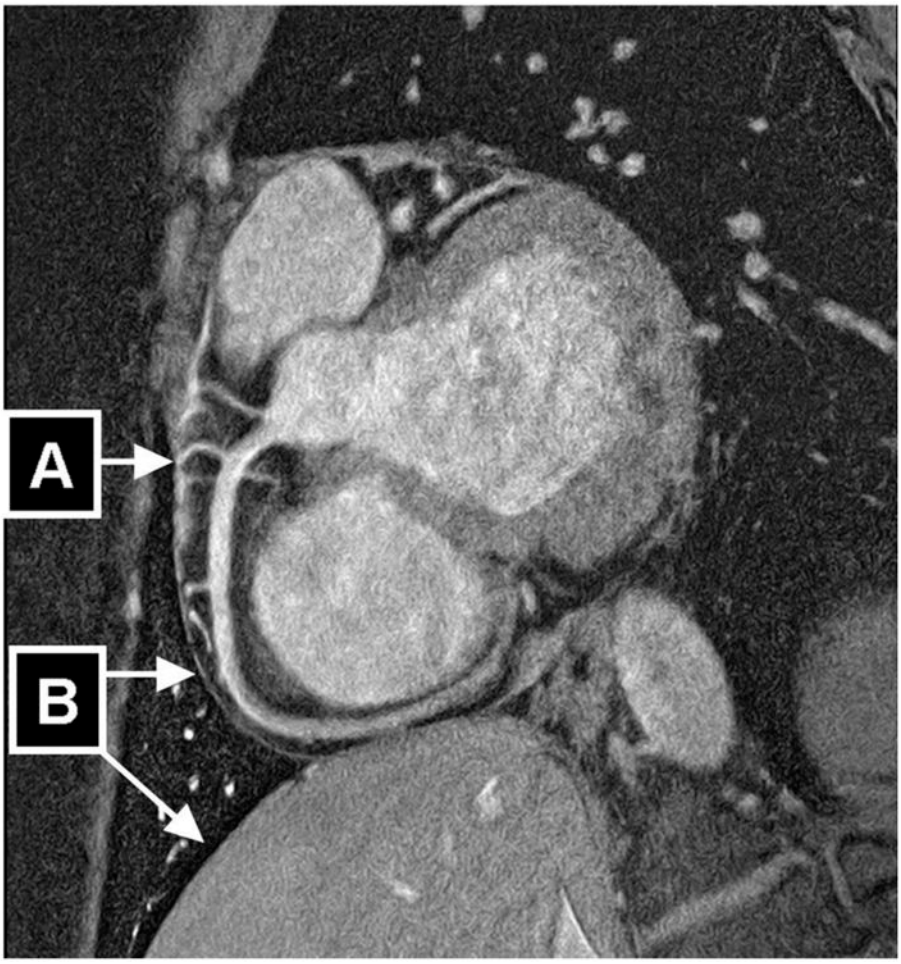

Figure 3.

Navigator-gated and navigator-corrected double oblique 3D segmented k-space gradient-echo imaging sequence (3 T, TR/TE = 7.5/2.3, α=20°, resolution=0.35×0.35×1.5 mm, field of view=270×216 mm, 800×610 matrix, scan duration = 906 seconds, 12 radiofrequency excitations per R-R interval, acquisition time window [T_{acq}] = 90 milliseconds, 10 slices [acquired], 20 slices [reconstructed], fat saturation). High-resolution scan of 23-year-old healthy man acquired at trigger delay of 591 milliseconds using FREEZE software tool (automated tool for the identification of the period of minimal myocardial motion) shows highly visible interface in region of coronary arteries (small-diameter branches [A]) as well as pericardium and lung-liver interface (B). Together with ability to reveal small-diameter branching vessels, this suggests excellent suppression of both intrinsic and extrinsic myocardial motion.

From: reference (42)

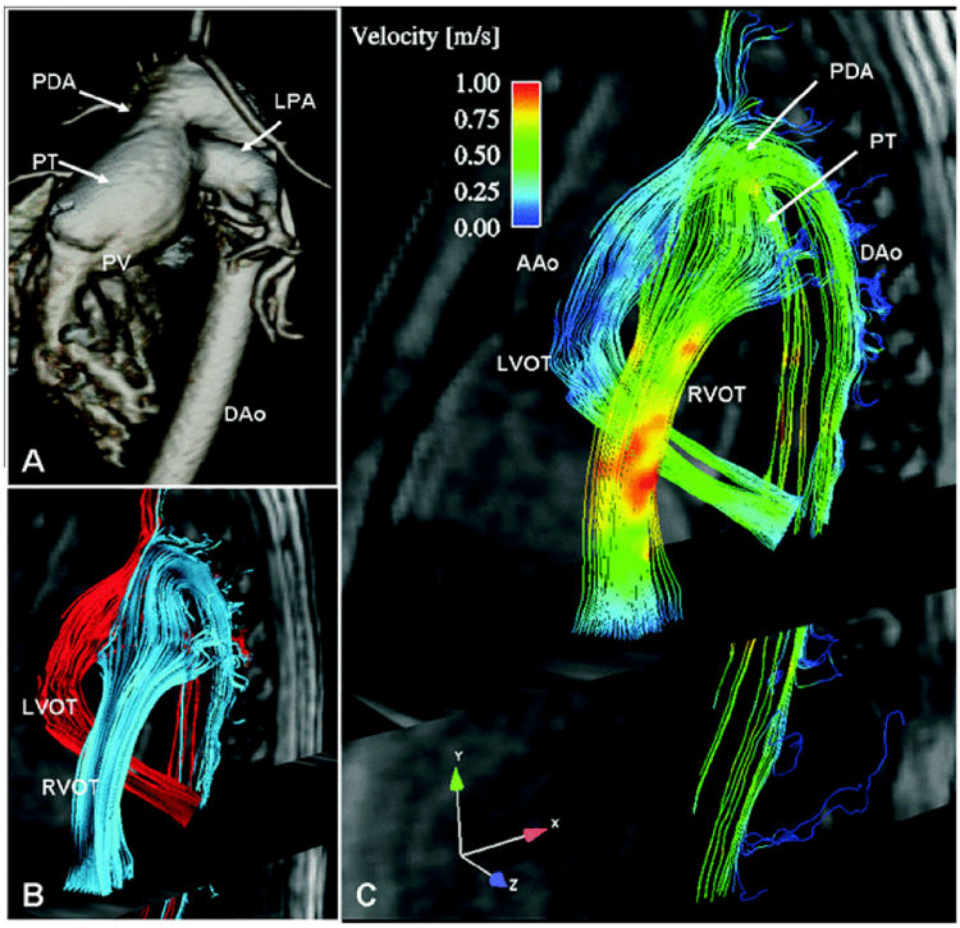

Figure 4.

Contrast enhanced CMR-angiography at 1.5T and volume rendered images of a large patent ductus arteriosus (PDA) between the dilated pulmonary trunk (PT) and the aorta. (PV = pulmonary valve, DAo = descending aorta, LPA = left pulmonary artery. B) Three-dimensional stream-lines originating from the left (LVOT, red) and from the right ventricular outflow tract (RVOT, blue). C) Color-coded 3D stream-lines demonstrating differences in flow velocities of the left and right outflow tract with the right ventricle predominantly contributing to aortic filling.

From: reference (53)

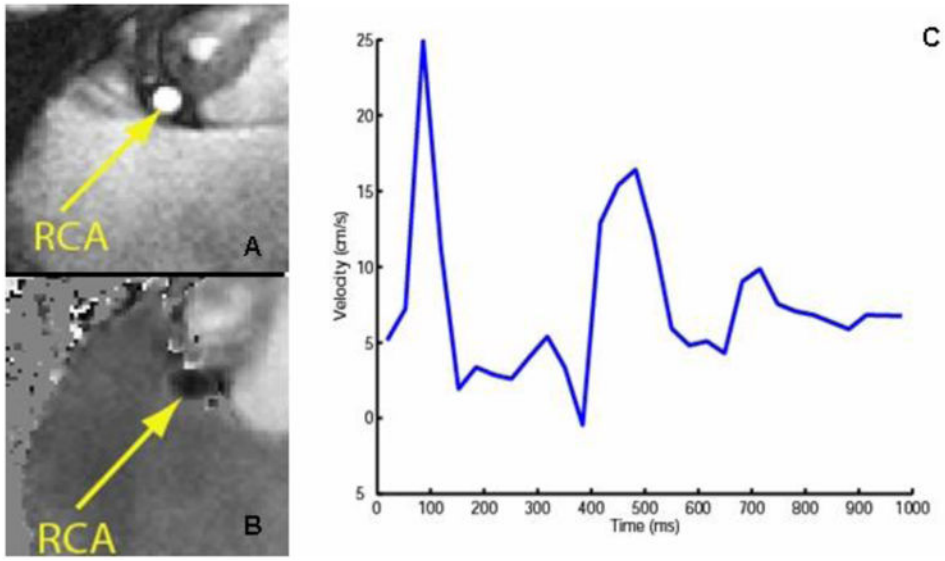

Figure 5.

Phase contrast imaging of the right coronary artery (RCA) (TR=5.2ms, TE= 2.8 ms, FOV = 280mm, matrix = 368, V_{ENC} =50 cm/s). Magnitude image (A) and flow map (B) through the RCA obtained at 3T. (C) Through plane blood velocity in the RCA measured during the cardiac cycle. (Image courtesy R. Nezafat and C. Stehning)